NASA TECHNICAL NOTE

NASA TN D-3535

C. 1

NASA TN D-3535

EXPERIMENTAL INVESTIGATION OF A HIGH-VOLTAGE ISOLATION DEVICE FOR ION-THRUSTOR PROPELLANT FEED

by Shigeo Nakanishi

Lewis Research Center

Cleveland, Ohio

NATIONAL AERONAUTICS AND SPACE ADMINISTRATION • WASHINGTON, D. C. • AUGUST 1966

EXPERIMENTAL INVESTIGATION OF A HIGH-VOLTAGE ISOLATION DEVICE FOR ION-THRUSTOR PROPELLANT FEED

By Shigeo Nakanishi

Lewis Research Center
Cleveland, Ohio

NATIONAL AERONAUTICS AND SPACE ADMINISTRATION

For sale by the Clearinghouse for Federal Scientific and Technical Information
Springfield, Virginia 22151 – Price $2.00

EXPERIMENTAL INVESTIGATION OF A HIGH-VOLTAGE ISOLATION DEVICE FOR ION-THRUSTOR PROPELLANT FEED

by Shigeo Nakanishi

Lewis Research Center

SUMMARY

This investigation extends the operating range of a high-voltage isolation device for the propellant-feed system of an ion thrustor. Some geometrical and operational parameters pertinent to electrical breakdown through the device (a nonconductive tube) are defined. Potentials to 10 000 volts were maintained within 14.6 centimeters of a grounded surface at a propellant flow rate of 14.2×10^{-4} gram per second and an estimated maximum tube pressure of 0.075 millimeter of mercury.

Ions from the thrustor are believed responsible for processes that lead to a breakdown. Deionizer pads with high ratios of surface area to volume were effective in reducing the leakage current through the tube. Two pads of low density were more effective than a single pad of high density. The locations of these pads relative to the ground electrode and to each other were significant factors in the critical voltage limit.

Comparison of a stainless-steel and a carbon ground electrode showed only minor differences in leakage current and breakdown voltage, which indicates that the secondary electron coefficient of these electrodes is of minor importance.

INTRODUCTION

The desirability of separating the high voltage of ion thrustors from the propellant-feed system becomes increasingly apparent when multimodular arrays of large thrustors are considered for long-term continuous operation. Systems requirements of propellant tankage, feed-rate control, and electrical isolation of individual thrustor modules fed from a common propellant source at space-vehicle ground potential can be met by using a high-voltage isolation device.

The feasibility of such an isolation device was demonstrated in a preliminary investi-

gation. The potential usefulness of the concept warranted a more complete evaluation. The present investigation studies the pertinent variables in order to determine the predominant operating parameters and to improve the performance of the device. The effects of pressure, electric field, and recombination surfaces within the vapor tube on the leakage current and the breakdown voltage were investigated.

The tests were conducted on a feed system attached to a 5-foot-diameter by 16-foot-long vacuum facility through a 12-inch gate valve. A 5-centimeter-diameter, electron-bombardment ion source was used with mercury as a propellant.

SYMBOLS

c, n	constants
d	interelectrode distance, cm
E	electric field, V/cm
J_E	filament or cathode emission current, A
J_L	leakage current to ground, A
J_N	equivalent mercury ion current, A
j	current density, A/sq cm
j_o	saturation photoelectric current density, A/sq cm
L_a	mean free path corresponding to average pressure, cm
ℓ	ground electrode to containment grid distance, cm
$\dot{m}$	nitrogen flow rate, g/sec
$\dot{m}_{Hg}$	mercury flow rate, g/sec
p	pressure, mm Hg
r	characteristic dimension of flow geometry, cm
S	deionizer pad to ground electrode distance, cm
V_I	net accelerating voltage, V
α	first Townsend coefficient
β	second Townsend coefficient
γ	ratio of Townsend coefficients, β/α

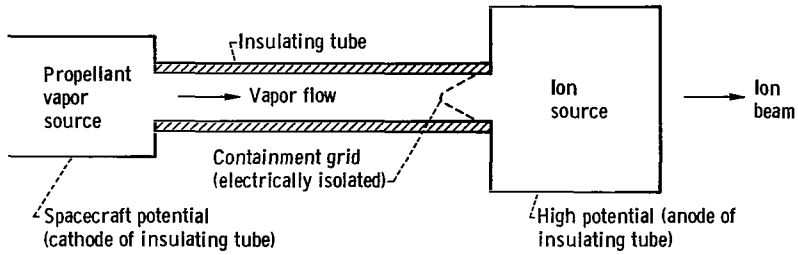

Figure 1. - High-voltage isolation device.

DESIGN CONSIDERATIONS

The basic design considerations of the high-voltage isolation device can be described by referring to figure 1. The insulating tube forms a flow channel between a source of propellant vapor and the ion source of the electron-bombardment thrustor. The vapor source operates at ground potential and the ion source at a high positive potential (2000 to 10 000 V) relative to ground. A plasma containment grid located upstream of the ion source inhibits the diffusion of charged particles into the vapor tube.

A preliminary experimental investigation showed high-voltage isolation capability to 6000 volts at a neutral propellant flow rate of 1.3×10^{-4} gram per second per square centimeter. Average tube pressure at the maximum flow condition investigated was estimated at 0.015 mm Hg. This pressure lies in the operating range of some mercury-arc tubes (ref. 1). With the onset of discharge at the critical breakdown voltage, the propellant tube becomes a mercury discharge tube operable at a low overall potential difference and at a current determined by the external circuit resistance. The basic problem in designing the isolation tube involves the prevention of the discharge over a wide range of tube pressure and voltage with an ion source already in operation at the anode (downstream) end of the tube. There also exists the possibility of transient arcs and electrical disturbances in the thrustor that may propagate into the otherwise quiescent vapor tube.

The specific mechanism of electrical breakdown in gases is not clearly understood. The primary process in all gaseous breakdowns, though, is the multiplication of electrons in a gas by cumulative ionization, which is caused by electrons advancing in the direction of the electric field. Secondary processes also occur that determine the threshold of the developing discharge (ref. 2).

Once a threshold is reached, a wide variety of breakdown forms may result. Whether the gap remains in a highly conducting state, such as an arc discharge, depends on the external circuit. In a thrustor system, power loss is usually minimized by using a low

external circuit resistance. This tends to drive the tube into a glow or arc-discharge mode once the threshold is reached and the breakdown is initiated.

For the present application, the threshold of breakdown is of prime concern. In much of the literature on direct-current breakdowns, reference is made to the Townsend theory and the criterion for a breakdown threshold. The Townsend equation,

$$\frac{j}{j_o} = \frac{(\alpha - \beta)e^{(\alpha-\beta)d}}{\alpha - \beta e^{(\alpha-\beta)d}} \tag{1}$$

relates a steady-state current density to the first and second Townsend coefficients that can be expressed in functional notation (ref. 1) as

$$\frac{\alpha}{p} = f\left(\frac{E}{p}\right) \tag{2}$$

and

$$\frac{\beta}{p} = g\left(\frac{E}{p}\right) \tag{3}$$

The steady-state equation (1) does not correctly describe the transient phenomenon of spark formation but does contain the mathematical condition that qualitatively implies a breakdown threshold; that is, when

$$\alpha = \beta e^{(\alpha-\beta)d} \tag{4}$$

the condition is attained wherein $j = \infty$ for $j_o \neq 0$, or j is indeterminate when $j_o = 0$. A more commonly encountered form of equation (1) is obtained by assuming that β is small relative to α and defining $\beta/\alpha = \gamma$. Then equation (1) becomes

$$\frac{j}{j_o} = \frac{e^{\alpha d}}{1 - \gamma e^{\alpha d}} \tag{5}$$

The condition,

$$\gamma e^{\alpha d} = 1 \tag{6}$$

sets the threshold for a self-sustaining discharge and is equivalent to equation (4) with the assumption and definition previously made.

The breakdown voltage, which experimentally is found to be a function of the parameter pd alone according to the Paschen law, can also be shown analytically from equations (2), (3), and (4) to be a function of only the same governing parameter (refs. 1 and 3). For carefully controlled experiments designed to obtain known uniform fields and known electrode conditions, the Paschen law of similitude is generally valid and tends to confirm the applicability of the Townsend theory. Inasmuch as the isolation device deals with breakdown and the prevention of it, the Townsend theory gives a qualitative understanding of the mechanisms and processes involved and formulates a basis for design.

The primary, or α, process alone cannot produce breakdown, and secondary mechanisms must be responsible for the onset of a self-sustaining discharge. In reference 4, a distinction is made between secondary processes in the gas and at the cathode by referring to β or γ processes, respectively. The secondary processes may result from metastable atoms, ionic collisions, photons, and other effects. At high electron and ion densities, space-charge effects may play an important role. The secondary process that predominates under specific conditions is difficult to determine. Factors such as space charge and electrode shape and condition may affect the breakdown voltage by creating nonuniformities in the electric field.

The existence of a continuous ion source was considered a major departure from the conventional gas discharge gap wherein the ions either exist from background ionization (photon, cosmic rays, etc.) or are created by the action of the primary process of electron impact. The generality of the threshold condition $\gamma e^{\alpha d} = 1$ is not precluded by the existence of a continuous ion source if the definition of γ is broadened to include the description of any number of processes which together yield the equivalent of a secondary action that determines the threshold condition. Hence, the breakdown voltage of the isolation device with the ion source operating compared with the breakdown voltage without the ion source operating could be interpreted as an indication of the strength of the secondary processes due to the ion source.

A design approach consisting primarily of maintaining the pressure and field within limits by providing sufficient flow conductance and appropriate tube length was used in the present investigation. The investigation was conducted in a series of comparative performance tests and observations. In particular, deionization media providing high ratios of surface area to volume were used to minimize the positive ion density and the ion bombardment of the ground electrode. A stainless-steel ground electrode and a carbon ground electrode were investigated to determine the effects of secondary electron yield from the electrode surface. The same thrustor was used throughout the investigation. The results presented herein should serve to evaluate the effects of configuration changes

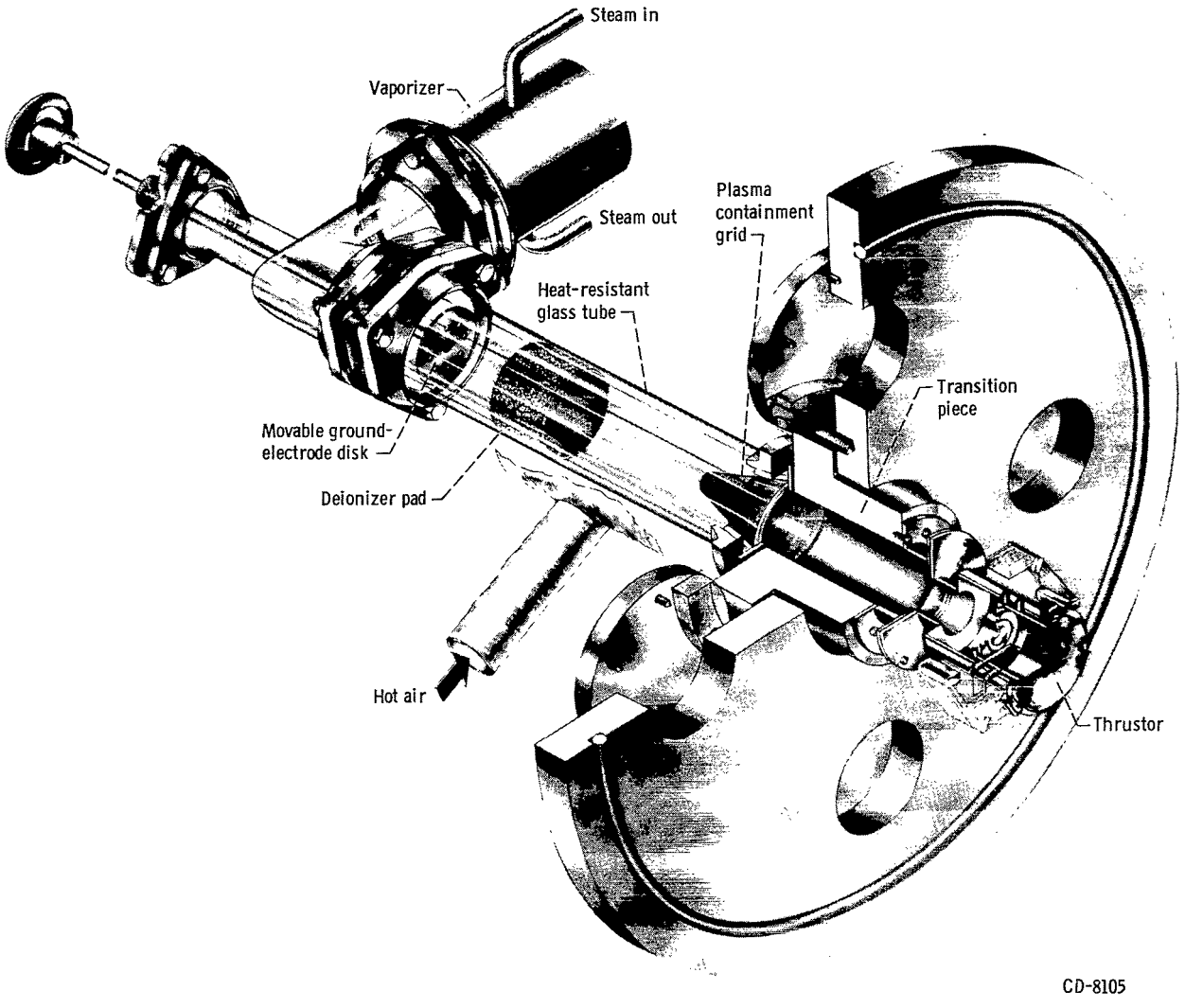

Figure 2. - Isolated mercury propellant feed system for electron-bombardment ion thrustor.

in the isolation device itself. A thrustor of significantly different design may, however, produce a different isolation capability.

APPARATUS

Propellant Feed System and Thrustor

The mercury propellant feed system and the electron-bombardment ion thrustor are shown in figure 2. The propellant duct consisted of 5-centimeter inside-diameter, heat-resistant-glass tubes with gasket seals. Mercury propellant vapor from a steam-heated

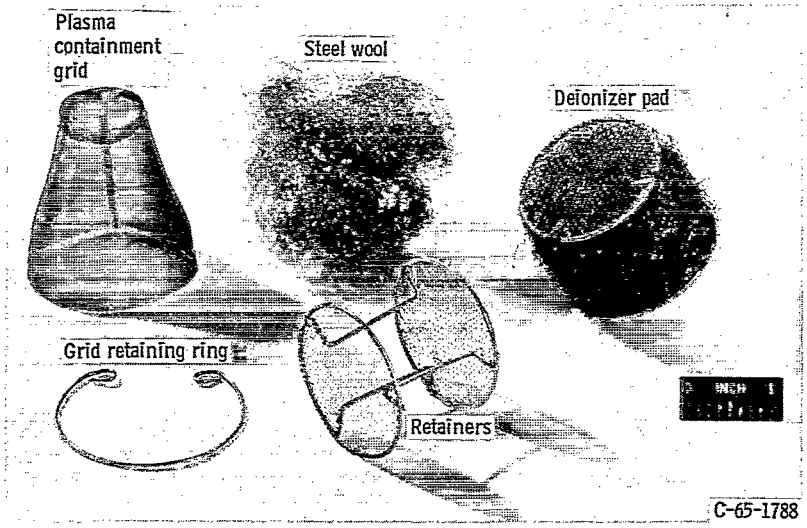

Figure 3. - Plasma containment grid and deionizer pad.

TABLE I. - DEIONIZER PAD DENSITIES

Thickness, cm	Density, g/cu cm
1.3	0.07
2.5	.07
3.8	.07
3.8	.10
3.8	.14

vaporizer fitted with an interchangeable calibrated orifice was fed into the side port of a glass tee upstream of a ground-electrode disk. The movable ground electrode was a 4.9-centimeter-diameter stainless-steel disk perforated with eight 3.2-millimeter-diameter holes. The disk was mounted on a rod that passed through a standard O-ring vacuum fitting on one of the straight ports of the tee.

Figure 2 shows the feed tube with a 3.8-centimeter-thick deionizer pad and a conical plasma-containment grid. A photograph of the grid, grid retaining ring, and pad is shown in figure 3. The pad was made by stuffing medium-grade steel wool between two circular retainers. The retainers consisted of 7-mesh-per-centimeter stainless-steel screening spot-welded on a wire ring and spaced by three support wires. The various pads used were stuffed as uniformly as possible to give the densities (weight of steel wool/volume) listed in table I.

The plasma containment grid was made from stainless-steel wire cloth fabricated from 0.077-millimeter wire woven at 42 mesh per centimeter. The developed area of the grid was about 83 square centimeters. Both the grid and pad were carefully fitted for tight seal between these components and the tube wall.

The propellant duct was connected to a transition piece of insulation material (polycarbonate resin). A 5-centimeter-diameter hole was bored through the transition piece, which provided a vacuum-tight flow passage for the propellant as well as a mount for isolating the thrustor from ground.

A 5-centimeter-diameter thrustor was used as the ion source throughout the investigation. Details of thrustor construction and operation are contained in references 5

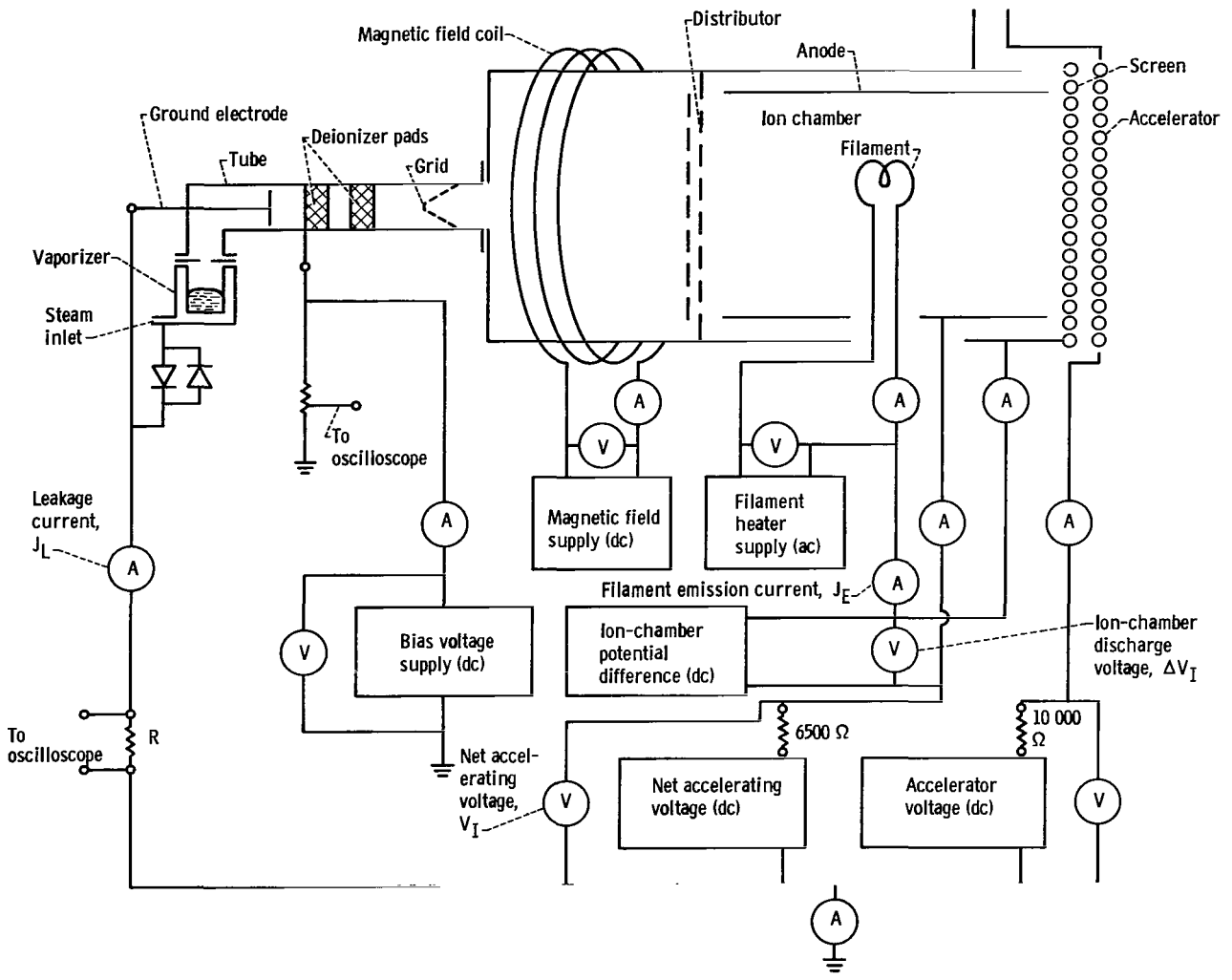

Figure 4. - Wiring diagram of ion thrustor and isolated propellant feed system.

and 6, which describe a 10-centimeter-diameter thrustor and its scaled-down counterpart, which was used herein.

The entire propellant duct and thrustor assembly was mounted on a 2.5-centimeter-thick, 50-centimeter-diameter aluminum flange that fitted over the port opening of a vacuum tank. Operation details of the vacuum tank are described in reference 5.

Hot air from an electrically heated blower was ducted around the glass tube to prevent propellant vapor condensation. The outer hot-air jacket that completely surrounded the propellant duct is only partly shown in figure 2. Steam was fed through neoprene hoses to isolate the vaporizer from ground. A pair of diodes connected the vaporizer to the ground electrode as a safety precaution.

Electrical System

A schematic wiring diagram of the thrustor and feed system is shown in figure 4 together with the instrumentation used in the investigation. The circuit and the power equipment used in thrustor operation were similar to those of the preliminary investigation. A 6500-ohm ballast resistor was inserted in the net accelerating voltage circuit to stabilize thrustor operation and to limit the current during a tube breakdown. The accelerator voltage circuit contained a 10 000-ohm ballast resistor for the same purpose.

Voltages of elements floating at high potential (e. g., deionizer pad) were measured by means of a 12 000-megohm voltage divider probe and a vacuum-tube voltmeter. Transient high voltages were measured by a 100-megohm voltage divider probe fed to an oscilloscope. Transient currents were recorded on an oscilloscope by feeding the voltage drop across a precision noninductive resistor R into a differential input amplifier.

PROCEDURE

Prior to the operation of the thrustor, a considerable preheat period was required to bring the glass tube, pad, and insulated transition piece to operating temperature (102° to 110° C) to avoid propellant condensation. A small quantity of water was fed through the vaporizer steam-jacket during preheat to prevent premature propellant flow.

Normal startup procedure for the thrustor was used after the preheat. Previously established check points of thrustor performance and background pressure were used as indications of the rated propellant flow for a given size orifice. Two orifice sizes were used in the present investigation. The smaller orifice had a 0. 183-centimeter diameter and yielded a nominal flow of 4.1×10^{-4} gram per second. The larger orifice had a 0. 356-centimeter diameter and yielded a nominal flow of 14.2×10^{-4} gram per second. The flow rate of each of the two orifices was determined by weighing the mercury propellant consumed during continuous 4-hour runs of actual thrustor operation. The vaporizer was maintained at a steam-jacket temperature of 99° C. The hot-air jacket of the propellant feed tube was held between 102° and 110° C throughout the runs.

The governing parameter for electrical breakdown pd was varied by changing the propellant flow rate, hence the tube pressure, and by changing the position of the ground electrode. The voltage at which electrical breakdown occurred through the tube (i. e., the critical voltage) was determined by increasing the net accelerating (or thrustor anode) voltage in steps of 500 or 1000 volts. The accelerator voltage was held at -2000 volts. Each voltage level was maintained long enough to record all the meter readings and to assure essentially equilibrium operation without a tube discharge.

Determination of a critical voltage was made at least twice to check repeatability.

In some instances, a tube breakdown would occur at a previously established stable condition. Such a point was generally 500 to 1000 volts below the critical voltage and was considered partly stable. Other test procedures peculiar to a particular phase of the investigation are discussed in the subsequent sections.

RESULTS AND DISCUSSION

Flow Characteristics

The difficulties involved in measuring mercury vapor pressure in the 10^{-3} to 10^{-1} mm Hg range led to inferring the flow characteristics of mercury vapor from the flow data of nitrogen gas. The flow rate of nitrogen was determined with a volume-displacement meter operating at a pressure of 15.7 pounds per square inch absolute and a temperature of 23° C. The nitrogen pressure at the upstream end of the insulating tube was measured by a calibrated thermal-conductivity pressure gage. The flow exhausted into the vacuum tank, which varied in pressure from 10^{-5} to 8×10^{-4} mm Hg depending on the flow rate. The measured pressure at the upstream end of the tube can thus be considered the pressure drop across the tube.

The nitrogen flow characteristics of various tube configurations are shown in figure 5. Comparison of the flow characteristics of the thrustor and transition piece (fig. 2) with those of other configurations indicated that the pressure drop occurred primarily across the isolation device. The nitrogen pressure drop through the thrustor and transition piece alone was essentially a linear function of flow rate as shown in figure 5(a). The thrustor had a 3.2-centimeter-diameter by 2.5-centimeter-long inlet tube that constituted a mild flow restriction. The pressure drop through a larger thrustor or a different inlet design might therefore be insignificant compared with the pressure drop through the isolation device.

Also shown in figure 5(a) is the calculated flow and pressure drop relation for a plain tube 45 centimeters long (without end corrections). The calculation assumed free molecular flow and a Clausing factor of 0.12 for a length-to-radius ratio of 18 (ref. 7). The pressure drop of the plain tube was also negligible compared with the pressure drop with pads.

The remaining configurations showed expected flow characteristics with the exception of the double-pad configuration. Both pads were 3.8 centimeters thick with approximately the same density (0.07 g/cu cm). A much higher pressure drop than that obtained experimentally was anticipated. The difference in flow characteristics resulting from the use of pads with a density of 0.10 gram per cubic centimeter was negligible.

The flow characteristics of selected configurations are plotted to logarithmic scale

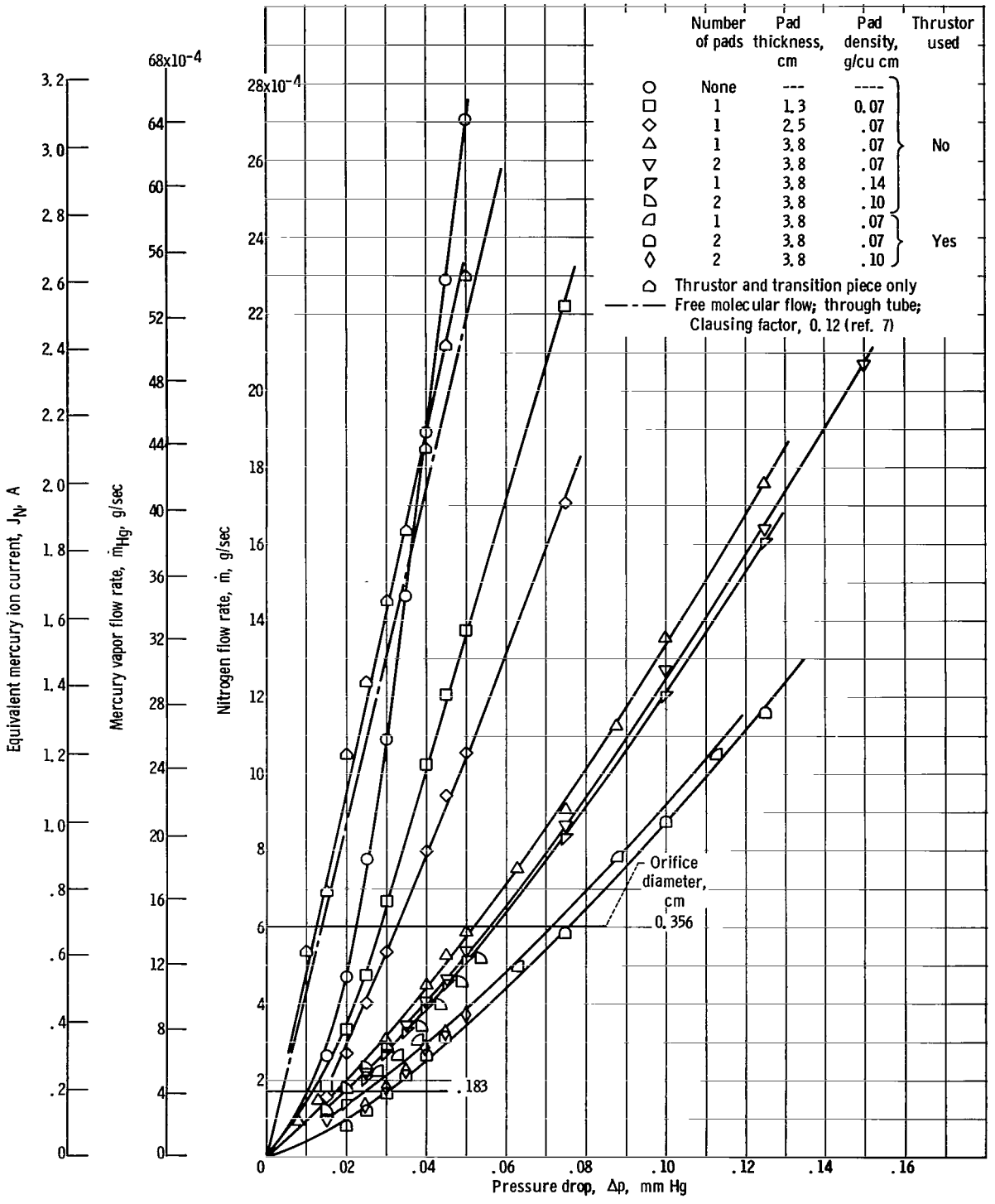

(a) Comparison of various configurations.

Figure 5. - Flow characteristics of propellant feed system components. Propellant duct, tube 5 centimeters in diameter by 45 centimeters long with containment grid.

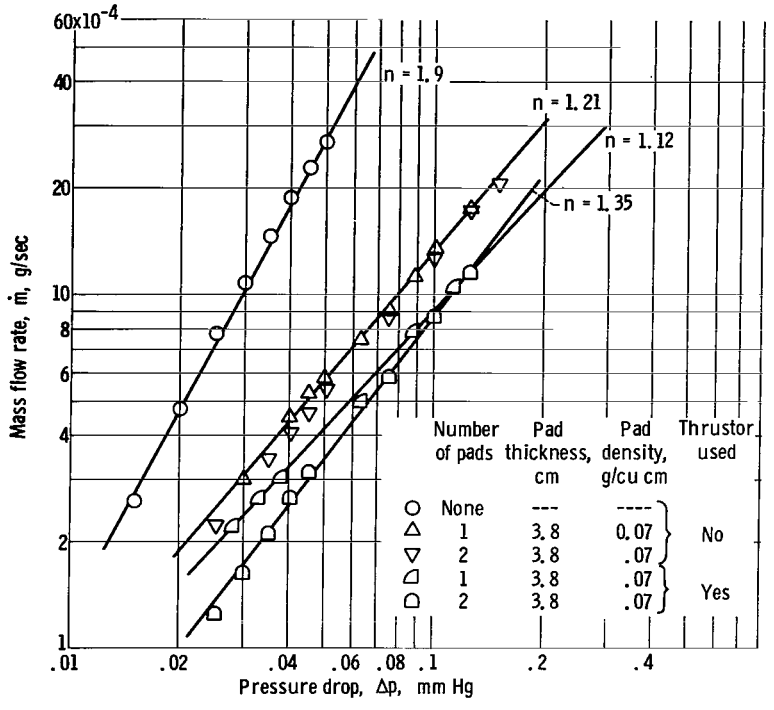

(b) Logarithmic plot of flow characteristics for selected configurations. Empirical equation, $\dot{m} = c\Delta p^{n}$.

Figure 5. - Concluded.

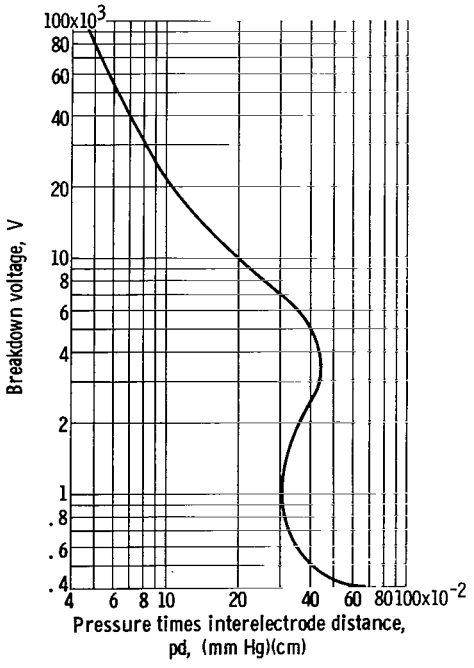

Figure 6. - Left branch of Paschen curve for mercury vapor. Interelectrode distance d, 3.8 centimeters (ref. 8).

in figure 5(b). The empirical equation fitting the data is $\dot{m} = c\ \Delta p^{n}$, wherein the exponent n defines the flow regime. Free molecular flow is indicated by $n = 1$, viscous by $n = 2$, and transition flow by $1 < n < 2$. The three flow regimes are also characterized by the Knudsen number L_a/r. On the basis of the empirical exponents, the flows of all configurations were in the transition region, with the flow through the pads showing more nearly free-molecular-flow characteristics. The mean free path in nitrogen for a pressure range of 0.01 to 0.1 mm Hg is approximately 1.0 to 0.1 centimeter. The mean pore sizes of the padded configurations are smaller than these dimensions, and therefore the Knudsen number corresponds to that of the near molecular flow regime. For the tube and grid configuration, the mean free path over an experimental pressure range of 0.015 to 0.05 mm Hg was from about 0.6 to 0.2 centimeter in a 2.5 centimeter-radius tube that also yields Knudsen

numbers in the transition range. The probable characteristic dimension of the grid (0.04- by 0.04-cm mesh opening) is smaller than the mean free path, but the data showed a transition flow regime because of the controlling (larger) magnitude of the tube pressure drop relative to the drop across the grid.

The nitrogen flow rate was multiplied by the factor

$$\left(\sqrt{\frac{\text{Temperature}}{\text{Molecular weight}}}\right)_{Hg}\left(\sqrt{\frac{\text{Molecular weight}}{\text{Temperature}}}\right)_{N_2}$$

to convert it to a mercury-vapor flow rate according to free-molecular-flow theory. The mass flow rate of mercury was in turn converted to an equivalent flow rate of singly charged mercury ions in amperes. The two converted scales are given in figure 5(a). The conversion to mercury flow may be slightly in error because the mean free path of mercury was about one-fourth that of nitrogen at the prevailing conditions. The net effect of a shorter mean free path should be less pressure drop for a given flow rate. The curves of figure 5(a), however, should indicate the pressure drops for mercury within about 10 percent according to some unpublished data.

Paschen Curve for Mercury Vapor

In the discussion to follow, frequent reference will be made to the Paschen curve of breakdown voltage in mercury vapor. The curve reproduced from reference 8 is shown in figure 6. The parameter pd that governs breakdown voltage is in units of (mm Hg)(cm). The data were obtained at a constant interelectrode distance of 3.8 centimeters, but the reference also presented other data to show the validity of the law of similitude for distances from 0.6 to 3.2 centimeters. Of the gases included in the data, only mercury, neon, and helium exhibited the nonmonotonic variation of breakdown voltage with pd as shown in figure 6 in the region where $pd < pd_{min}$ (i.e., the left branch). Data beyond a pd value of 0.6 were not available. The right branch of the curve probably begins at about this value of pd, but this region is outside the range of interest in the present investigation.

Tube and Grid Configuration

Results obtained with a configuration consisting of the propellant feed tube, the plasma containment grid, and the thrustor are shown in figure 7. The propellant flow

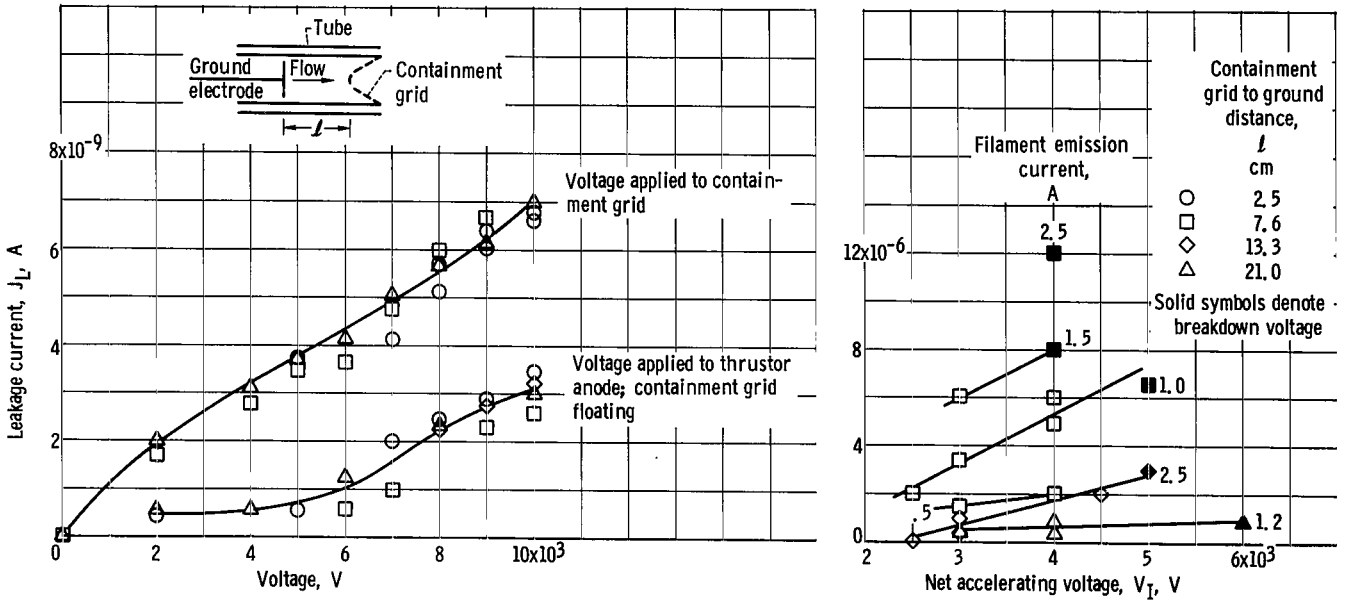

(a) Thrustor not operating.

(b) Thrustor operating.

Figure 7. - Leakage current of tube and containment grid. Propellant flow rate, $4.1x10^{-4}$ gram per second.

rate was 4.1×10^{-4} gram per second. Figure 7(a) shows the leakage current through the ground electrode circuit obtained by applying the positive potential either to the thrustor anode or to the containment grid with the propellant flowing and the thrustor not operating. No electrical breakdown was encountered up to the arbitrarily established voltage limit of 10 000 volts at any of the interelectrode distances investigated.

The uniform-field Paschen curve for mercury vapor (fig. 6) shows a breakdown voltage of 10 000 volts at a value of pd of 0.2 (mm Hg)(cm). With a grid to ground electrode distance of 21 centimeters in the propellant tube, the pressure required for breakdown at 10 000 volts would be about 0.01 mm Hg. The pressure drop for the tube and grid configuration shown in figure 5(a) was for a tube length of 45 centimeters. With a 21-centimeter tube and the thrustor, the maximum tube pressure in the upstream region may be as high as 0.008 mm Hg, but between the electrodes, the average pressure was probably about 0.004 to 0.006 mm Hg. The value of pd should thus be well below that for breakdown, which agrees with the results obtained. Of course, the conditions of nonuniform pressure and possibly a nonuniform electric field make such comparisons approximate.

From the Townsend breakdown criterion (eq. (4)), it may be concluded that the value of β was less than the critical value and perhaps vanishingly small inasmuch as no breakdown was encountered to 10 000 volts. According to equation (1), the steady-state current should thus vary as $e^{\alpha d}$. The leakage current shown in figure 7(a) was in the 10^{-9} ampere level, and the current was higher when the potential was applied to the grid rather than to the thrustor anode. In either case, no strongly defined trend of leakage current with distance was found. At a given distance, however, the leakage current increased with electric field, or voltage. This trend implies that the value of α increased with electric field in accordance with equation (2). Limited available data for mercury vapor show that α/p initially increases with E/p but attains a maximum and decreases at higher values of E/p. The nonuniformity in the tube pressure and the unknown electric field distribution along the tube length together with the unknown function $f(E/p)$ again make a precise comparison with the theory difficult and questionable.

The leakage current obtained at three grid to ground distances with the thrustor in operation is shown in figure 7(b). The current level was generally three orders of magnitude higher than that obtained with the thrustor not operating. The numerals affixed on the curves are average values of filament emission current in amperes. The critical voltage at which a breakdown discharge occurred through the tube is indicated by a solid symbol. At the 21 centimeters distance, the leakage current was less than 1 microampere and the critical voltage was 6000 volts, which agreed with the general values found in the preliminary investigation. The breakdown point was usually the terminal point in a gradually increasing leakage current, but there was no observable rise in the steady-state current just prior to breakdown. The level of the steady-state

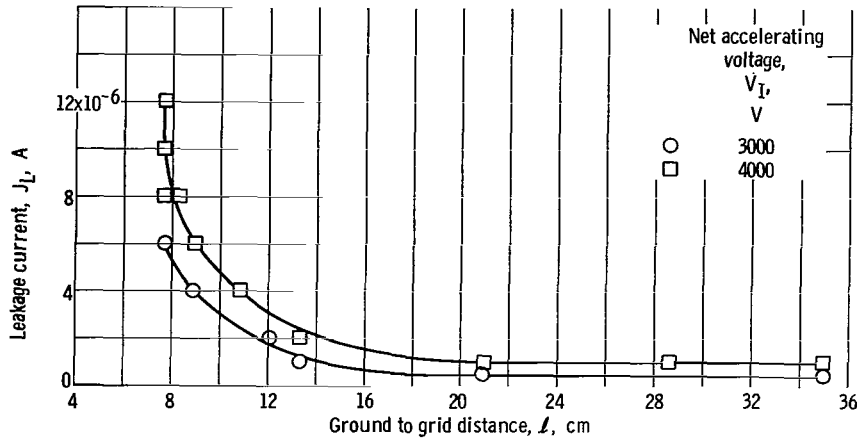

Figure 8. - Effect of ground to containment grid distance on leakage current of tube and containment grid. Filament emission current, 1.5 amperes; propellant flow rate, $4.1x10^{-4}$ gram per second.

leakage current in itself was not a precursor to a tube breakdown. Breakdowns occurred with explosive suddenness at leakage currents considerably lower than those of some other stable operating conditions.

The voltage on the containment grid was not measured in the present investigation but was less than 50 volts negative with respect to the net accelerating voltage in the preliminary investigation. For small leakage currents, the containment grid may be considered the anode of a discharge gap equal to the grid to ground distance ℓ inasmuch as the floating grid potential is approximately equal to the net accelerating voltage.

If the pressure in the tube is, at most, 0.010 mm Hg, the product of pressure and distance pd is 0.21, 0.13, and 0.076 for the grid to ground distances of 21, 13.3, and 7.6 centimeters, respectively. The Paschen curve of figure 6 gives breakdown voltages of 10 000 volts and higher for these three values of pd. The conventional Paschen curve apparently does not apply to the present configuration in the presence of an ion source. In fact, the breakdown voltages decreased rather than increased with decreasing distance as the Paschen law indicates for this region of pd. Examined in the light of the Townsend theory, the present results are not incompatible with the theory if the presence of additional secondary mechanisms is allowed. Without specifying which of the secondary mechanisms are predominating, a breakdown threshold condition can be made compatible with equation (6) by postulating increases in β or γ.

The variation in leakage current with ground to grid distance is shown in figure 8. Filament emission current was held constant at 1.5 amperes for the two voltages shown. Beyond a distance of about 15 centimeters the leakage current was practically independent of distance. The rapid rise in current below 15 centimeters ground to grid distance may possibly be due to a higher rate of ion leakage from the plasma containment grid and less ions lost by diffusion (smaller wall area). The rise in current cannot be satisfactorily

explained in terms of vacuum space-charge flow because calculated vacuum space-charge currents are one to two orders of magnitude larger than the measured currents.

The effect of filament emission current on the leakage current is shown in figure 9. At very low emission currents, the leakage was low even at short ground to grid distances. This is probably because of the low plasma density in the thrustor. The leakage current increased with emission current for the short ground to grid distance but was essentially independent of emission current for 13.3 centimeters and greater distances as can be inferred from figure 8.

Results obtained with the tube and grid configuration showed only limited high voltage isolation capability, even at low tube pressures. Beyond a minimum limiting distance, increasing the length of the isolation tube did not reduce the leakage current proportionately. The electrical breakdowns occurred only when the ion source was in operation.

Single Deionizer Pad Configuration

Recombination of the charged particles to form neutral atoms was sought as a means to reduce the leakge current through the propellant tube. High leakage current was assumed to be undesirable from the standpoint of increasing the probability of secondary mechanisms or of establishing a highly nonuniform electric field along the tube length. The low rate of volume recombination expected at low pressures required the use of a large surface area to enhance surface recombination.

A single pad, 3.8 centimeters thick with a density of 0.07 gram per cubic centimeter, was placed 11.4 centimeters upstream of the tip of the containment grid. The leakage current and critical voltages obtained at a propellant flow rate of 4.1×10^{-4} gram per second are shown in figure 10(a). The filament emission current was held constant at 2 amperes. The pad to ground distance S was measured from the ground electrode to the upstream face of the pad (see fig. 10). At S = 0, that is, with the ground electrode contacting the pad, the minimum distance between the containment grid and a grounded surface was 11.4 centimeters. Stable operation to 10 000 volts was possible with this configuration. The leakage current rose rapidly at short pad to ground distances, as in the case with no pad. Leakage currents with and without the pad at a grid to ground distance of 21 centimeters were about equal. Likewise, at S = 0 (fig. 10) and ℓ = 11.4 centimeters (fig. 8), the leakage currents were similar. The significant difference was the extended range of operating voltages at leakage currents higher than those at which breakdown was previously encountered. The absence of breakdown at S = 0 was unexpected. Although the pad was at ground potential when S = 0, the use of a pad and the more uniform distribution of mercury vapor over the entire cross-sectional area of the

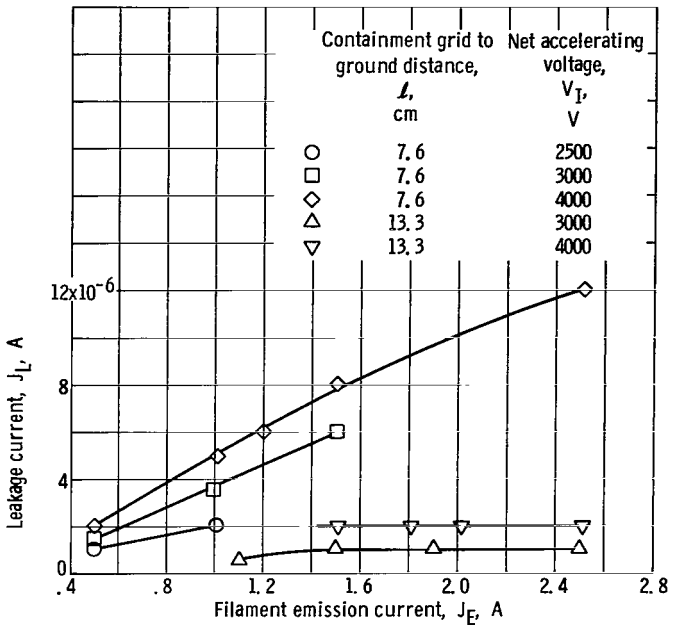

Figure 9. - Effect of filament emission current on leakage current of tube and containment grid. Propellant flow rate, 4.1x10^{-4} gram per second.

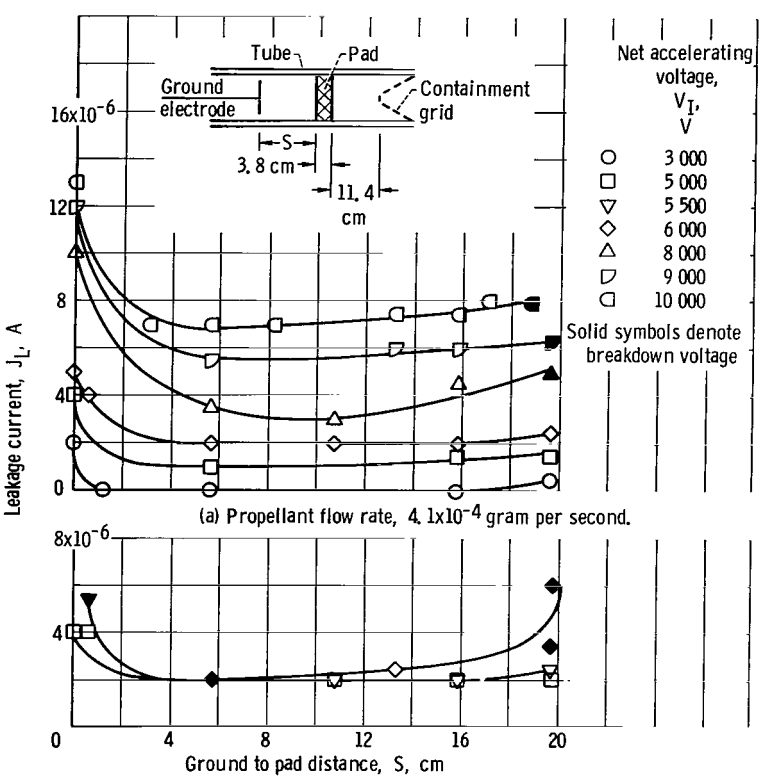

Figure 10. - Performance of single-pad configuration. Filament emission current, 2.0 amperes.

tube may be a contributing factor. The stainless-steel movable ground electrode had eight holes through which the mercury vapor flowed to produce local regions of high number density and perhaps preferential arc seats at the grounded surface. The floating potential of the pad was not measured at this phase of the investigation. A subsequent section of the report presents typical values of pad potential.

The reason for breakdowns encountered at S = 19 to 20 centimeters and net accelerating voltages of 8000 volts or above was not ascertained. When a tube pressure of 0.025 mm Hg (fig. 5) is assumed, the value of pd (or pS) is 0.475 to 0.5 (mm Hg)(cm). The breakdown voltages predicted by the Paschen curve at these distances are below 1000 volts. In the present configuration, no breakdown occurred for voltages from 3000 to 6000 volts. At each level of net accelerating voltage, however, the leakage current as a function of ground to pad distance showed a minimum. Increasing distances and longer ionizing path lengths possibly contributed to both the primary and secondary processes, hence, an increase in the leakage current.

The single pad configuration was also operated at the higher propellant flow rate of 14.2×10^{-4} gram per second, and the results are shown in figure 10(b). The operable voltage range was reduced although leakage current was not greatly different from that obtained previously. A pad to ground distance of about 10 or 13 centimeters appeared to be near optimum at a net accelerating voltage of 6000 volts. Tube breakdowns were encountered at 6000 volts for distances much larger or smaller than the optimum. The effects of different propellant flow rates having been briefly determined, it appeared that the relative merits of other configurations could be evaluated using the 14.2×10^{-4} gram per second flow rate and the associated tube pressure as a point of reference. For the remainder of the investigation, therefore, this propellant flow rate was used.

Prior to the evaluation of a two-pad configuration, a single 3.8-centimeter-thick pad of high density (0.14 g/cu cm) was investigated. The critical voltage limits obtained were 6500 to 7000 volts, which were only slightly higher than the limits obtained by using a pad with a density of 0.07 gram per cubic centimeter.

Double Pad Configurations

Two configurations utilizing double pads were investigated. The first configuration consisted of two pads in series, each 3.8 centimeters thick with a density of 0.07 gram per cubic centimeter. The location of the components are shown in the inset of figure 11. The downstream pad was located with the downstream surface 14 centimeters from the tip of the containment grid. With a space of 3.8 centimeters between the two pads, the overall assembly measured 25.4 centimeters from the tip of the containment grid to the upstream face of the rear pad. A thin conductor was connected to the rear pad and led

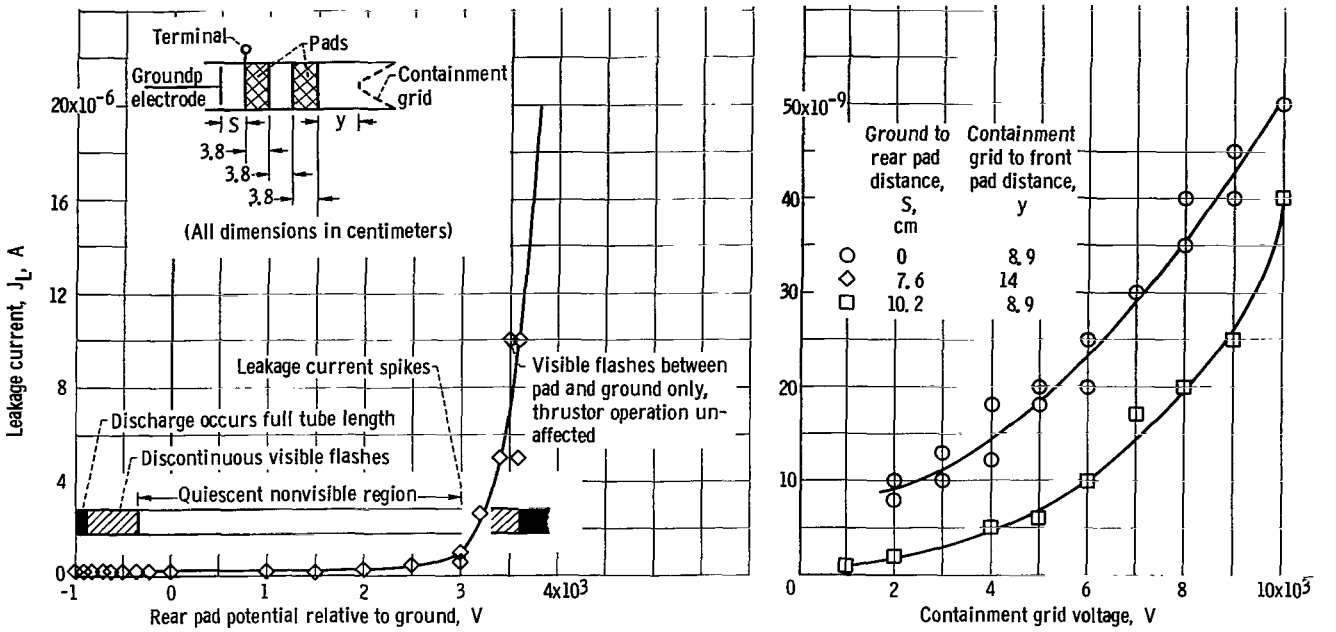

(a) Filament emission current, 2.0 amperes; net accelerating voltage, 5000 volts; accelerator voltage, -2000 volts; pad density, 0.07 gram per cubic centimeter.

(b) Thrustor not operating; pad density, 0.10 gram per cubic centimeter.

Figure 11. - Effects of rear pad potential and containment grid voltage on leakage current. Propellant flow rate, 14.2×10^{-4} gram per second.

out between two flange gaskets to provide an insulated terminal.

A range of bias voltage was applied to the rear pad. The resulting effects on tube discharge characteristics are shown in figure 11(a). The bias voltage was measured relative to ground. The net accelerating voltage was maintained at 5000 volts, the filament emission current at 2 amperes, and the ground to rear pad distance at 7.6 centimeters. This condition is completely stable as attested by a flow calibration run of 4 hours duration without a single tube breakdown.

A broad range of rear pad bias voltage from -350 to 3000 volts produced relatively little change in leakage current, and the entire tube was quiescent with no visible glow. Leakage current through the ground electrode circuit was about 0.2 microampere. As the rear pad bias voltage approached the neighborhood of 3000 volts, the leakage current increased. Current spikes were detectable on the leakage current meter. Further increase in pad bias voltage beyond 3400 volts caused a rapid rise in leakage current and visible discharges. These discharges occurred between the rear pad and the ground but not between the forward pad and the containment grid. The circuit breaker in the bias power supply opened when a visible discharge occurred. Occasionally, the discharge between the pad and the ground electrode continued momentarily even after the bias supply circuit breaker opened. During these discharges, however, the ion source continued operating at 5000 volts with no apparent effects. The increase in rear pad voltage, and hence in the electric field between pad and ground, caused a transition to a visible discharge that did not propagate toward the thrustor.

The measured current of the visible discharge was considerably higher than might be expected from a normal glow discharge. A meter on the bias power supply indicated steady-state currents as high as 60 microamperes and current spikes up to 200 microamperes. With an initially applied bias voltage of 3500 volts or more, the discharge probably developed into the abnormal glow discharge. When the power supply breaker opened, there was no energy source except possibly the output filter circuit that supplied a transient discharge current until the energy was fully dissipated.

A high negative bias produced a different behavior. As the negative bias voltage was increased beyond 350 volts, intermittent visible flashes occurred between the downstream pad and the containment grid. The leakage current through the ground electrode remained constant, and the meter in the bias supply showed no response. At about -900 to -1000 volts, the previously intermittent discharge suddenly became continuous and extended the full length of the tube. The circuit breakers of both the bias power supply and the net accelerating voltage power supply opened shortly thereafter. The discharge extended to the ground electrode possibly because, with the bias supply circuit breaker open, the rear pad voltage immediately rose to a value sufficiently high to establish a discharge in the ground-to-rear-pad region. The overall potential difference between the thrustor net accelerating voltage and the rear pad negative bias voltage at the onset of discharge was about 6000 volts. This was approximately the critical voltage obtained with the single-pad configuration at a similar ground-to-pad distance.

The second double pad configuration was identical to the first except for a pad density of 0.10 gram per cubic centimeter and an 8.9 centimeter grid-to-downstream-pad distance (see inset, fig. 11). With the propellant flowing but thrustor inoperative, the positive potential was applied to the containment grid. The leakage current thus obtained at two ground to rear pad distances are shown in figure 11(b). At the tube pressure corresponding to the propellant flow rate of 14.2×10^{-4} gram per second (about 0.075 mm Hg), the maximum leakage current was 50×10^{-9} ampere. Up to the maximum applied voltage of 10 000 volts, no breakdown was encountered even with the rear pad grounded. The absence of breakdown without thrustor operation, and conversely, the connection between the operation of the thrustor ion source and breakdown was thus confirmed again (see section Tube and Grid Configuration).

Thrustor operation at elevated potentials appeared possible if the following conditons could be satisfied:

(1) Two pads of moderately high density should reduce the ion population in the region between ground and rear pad so that the ion density is close to that obtained without thrustor operation.

(2) The potential difference between the containment grid and the rear (upstream) pad should be held below the critical value of 6000 volts corresponding to the -1000 volts bias condition shown in figure 11(a).

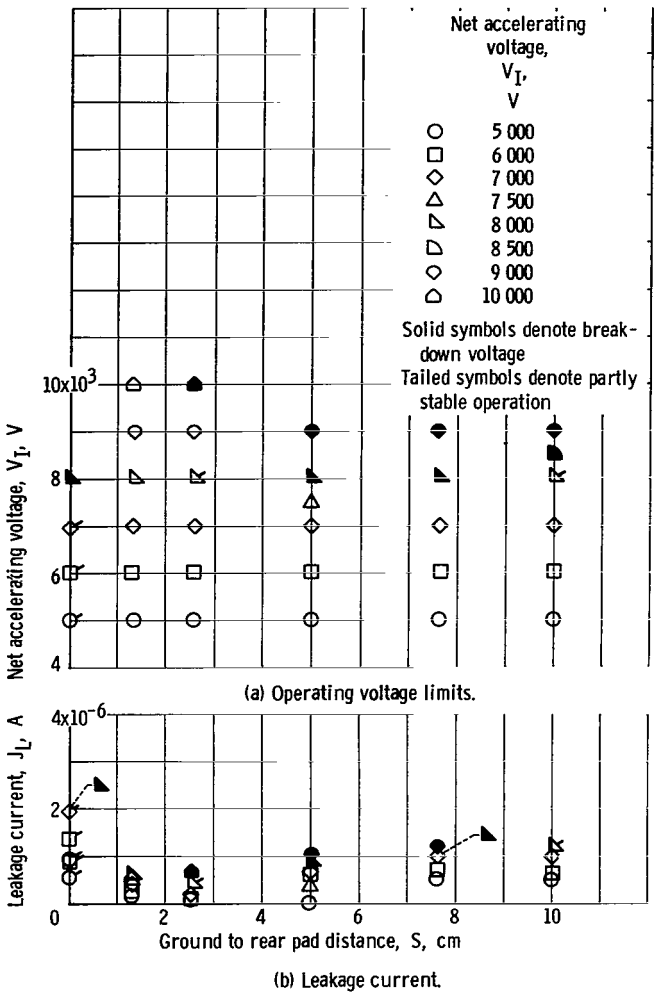

Figure 12. - Performance of double pad configuration. Propellant flow rate, $14.2x10^{-4}$ gram per second; filament emission current, 1.5 amperes; front pad to containment grid distance, 8.9 centimeters.

(3) In the region where pressure is highest, the breakdown parameter pd should be small (i.e., the ground-to-rear-pad distance S should be an optimally small value determined experimentally).

The operational range obtainable with the double pad configuration was determined at various ground-to-rear-pad distances. Both pads were isolated to determine the isolation capability of the configuration operated in this mode. Filament emission current was held at 1.5 amperes. A limited amount of operation was performed at a filament emission current of 2 amperes with no derating in the isolation capability. As shown in figure 12(a), no breakdown was encountered to 10 000 volts at a ground-to-rear-pad distance of 1.3 centimeters. When the ground electrode contacted the rear pad, the configuration reverted to a single pad configuration, and the operation became only partly stable above 5000 volts.

The leakage current is shown in figure 12(b). The trend of an increased current at a ground-to-pad distance of zero and at very large distances was again evident. The general level of the current was lower than that of the single pad configuration, but higher by three orders of magnitude than that obtained with the thrustor inoperative.

Effect of Component Distances

A performance comparison of four configurations in which the ground-to-rear-pad distance was held constant at 1.3 centimeters is shown in figure 13. Configurations A to C were double-pad configurations. Configuration D was a single-pad configuration formed by removing the forward (downstream) pad.

The potential of the pad immediately adjacent to the ground electrode is shown in

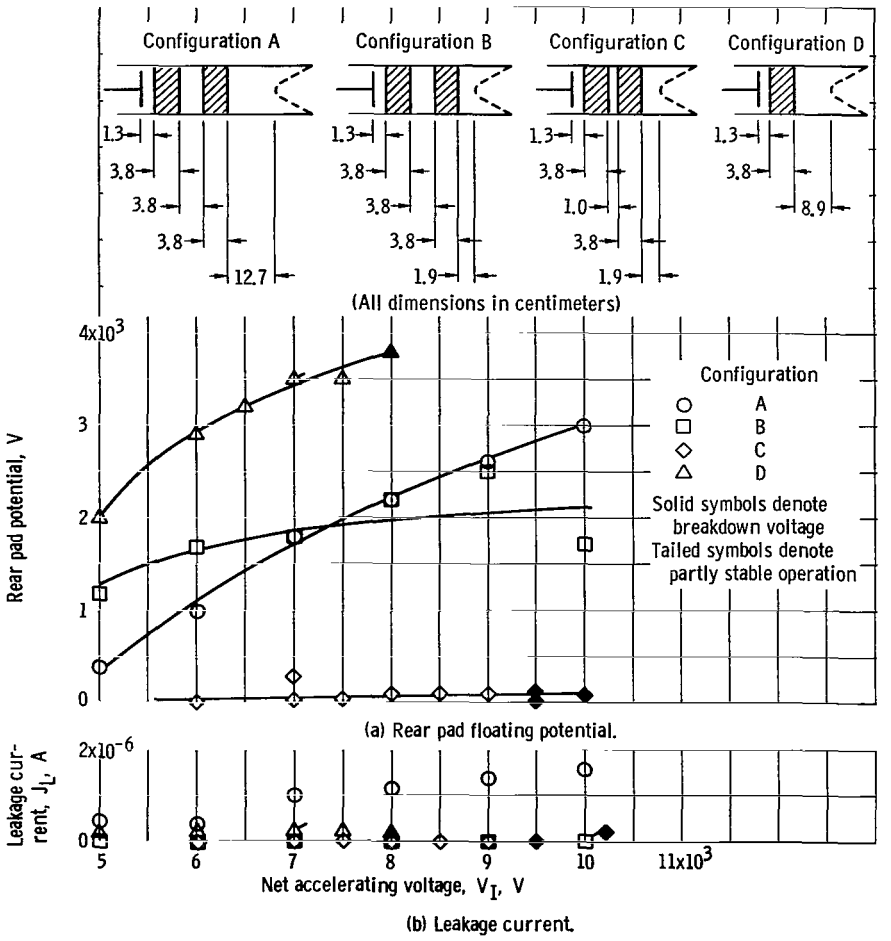

Figure 13. - Performance comparison of pad configurations. Propellant flow rate, 14.2x10^{-4} gram per second; filament emission current, 1.5 amperes; distance from ground electrode to rear pad, 1.3 centimeters.

figure 13(a). Configurations A and B, which had the same pad-to-pad distance but widely different containment grid-to-pad distances, resulted in approximately the same rear pad potential. No breakdown was encountered with net accelerating voltages to 10 000 volts. With the pad-to-pad distance reduced to 1 centimeter in configuration C, the rear pad potential remained near zero, but breakdowns were encountered at 9500 and 10 000 volts. The comparison of these three configurations seems to indicate that because the pressure in the containment grid-to-forward-pad region is low, (long mean free path), a broad range of grid-to-pad distance is tolerable. In the region of higher pressure, the increased probability in occurrence of secondary mechanisms requires that the pad-to-pad distance be a compromise based on electric field and ionizing path length.

Configuration D, which consisted of a single pad, resulted in pad potentials 1000 to 2000 volts higher than those obtained with an additional pad present. Breakdown

occurred at 7000 and 8000 volts.

The leakage currents obtained with the four configurations are shown in figure 13(b). Little or no leakage current was assumed beneficial, yet breakdown occurred with leakage currents less than 1 microampere if the rear pad-to-ground electrode distance exceeded 1.3 centimeters (fig. 12). Breakdown at low current also occurred in the absence of a second pad regardless of the 1.3-centimeter distance. The use of two pads is necessary to increase recombination and to avoid a locally high electric field distribution along the tube length.

Preventing the backward flow of ions or minimizing the ion population in the ground electrode region is necessary for the successful application of the Paschen law of similitude for gaseous breakdown. The use of a second pad is indicated in preference to a single pad of high density. An additional requirement is that the potential gradient along the tube be such that no region exceeds the breakdown field corresponding to the local pressure and ion density. Ramifications of the design principles are undoubtedly possible. Accurate prediction of what the design changes will do, however, may require a better understanding of the intrinsic nature of the secondary mechanisms that are necessary for the onset of a self-sustaining discharge.

Low Secondary Emission from Ground Electrode

With the onset of an electrical breakdown in the tube, sufficient electron emission from the ground electrode is usually required to sustain a continuous discharge. A ground electrode material possessing a low secondary yield of electrons per incident ion might thus increase the critical voltage limit.

A limited amount of data on electron yield is given in reference 4 for mercury gas with iron electrodes. Data on stainless steel and other materials were not available. Secondary electron emission by electron bombardment is reported more extensively in the literature. If a similar correspondence in relative yields is assumed, the maximum secondary electron yield from carbon could be about 23 percent lower than from iron or nickel. The yield from an iron electrode in mercury gas at values of E/p from 800 to 1400 volts per centimeter per mm Hg is about 10^{-5} electron per positive ion. In the rear pad-to-ground region of the tube, the value of E/p was about 2600 to 3500 volts per centimeter per mm Hg, but the yield is not expected to be much different at these higher fields because of the trend of the yield curve. In view of the low yield, the effect of electrode material on breakdown voltage may be negligible. Electron emission is nevertheless a type of secondary process occurring at the cathode. As shown in equation (6), because of the exponential term $e^{\alpha d}$, γ need not be large to satisfy the threshold condition.

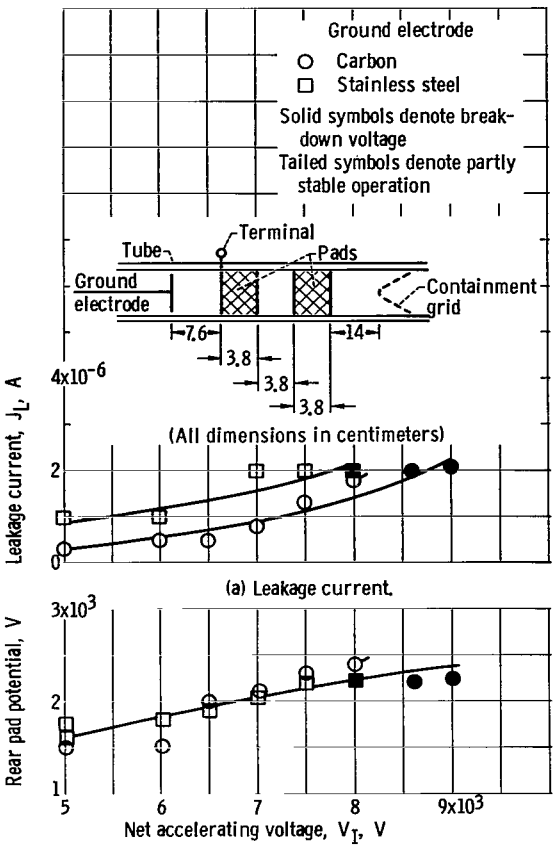

Figure 14. - Effect of ground electrode material. Propellant flow rate, $14.2x10^{-4}$ gram per second; filament emission current, 1.5 amperes.

A ground electrode disk geometrically similar to the stainless-steel disk described in the section APPARATUS was fabricated of 3.1-millimeter-thick carbon and located 7.6 centimeters upstream of the upstream pad (see inset, fig. 14). This ground-to-pad distance was chosen to obtain breakdowns near 8000 volts. Care was taken to expose no metallic surface on the face of the disk.

The leakage currents obtained with the two electrode materials are shown in figure 14(a) as a function of net accelerating voltage. The leakage with the carbon electrode was approximately 0.5 microampere lower than that of the stainless-steel electrode over the entire voltage range. Because of the low yield value (10^{-5}), a 1-microampere current of secondary electrons would require an unreasonably high ion current on the order of 0.1 ampere. The observed leakage current may thus be an ion collection current at the ground electrode rather than secondary emission. The critical voltage was not significantly different. Conclusions regarding the secondary yields of these two electrode materials should be made with caution. As stated in reference 1, electron emission by positive ion bombardment is markedly affected by the condition of the cathode surface and contamination by foreign materials and gases (particularly mercury vapor).

The rear pad potentials associated with the two electrodes are shown in figure 14(b). The magnitude and trend of potential were similar to those of configurations A and B shown in figure 13(a). No consistent difference in potential as a result of electrode material was evident. If secondary emission is negligible and pad potential is essentially a function of processes occurring between the ion source and the rear pad, electrode material can have little effect upon the rear pad potential. This fact is particularly true if the secondary emission effect of the electrode material is masked by the effect of the mercury vapor that is present at both electrodes.

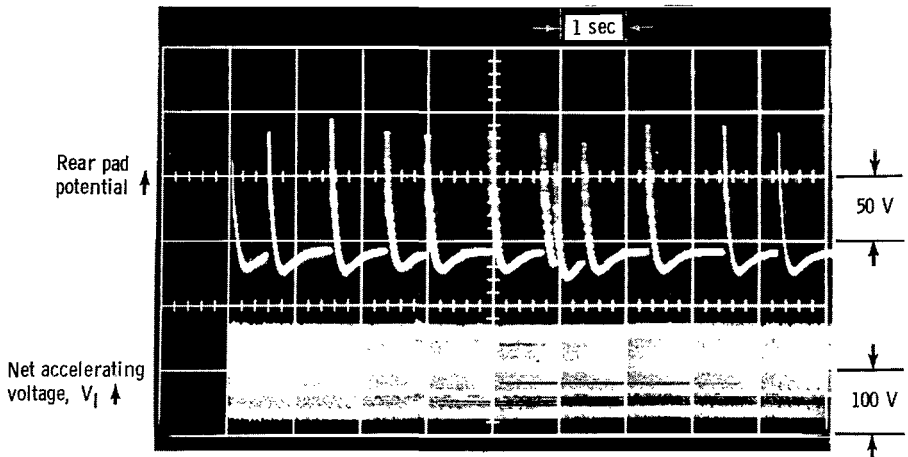

(a) Sweep rate, 1 centimeter per second.

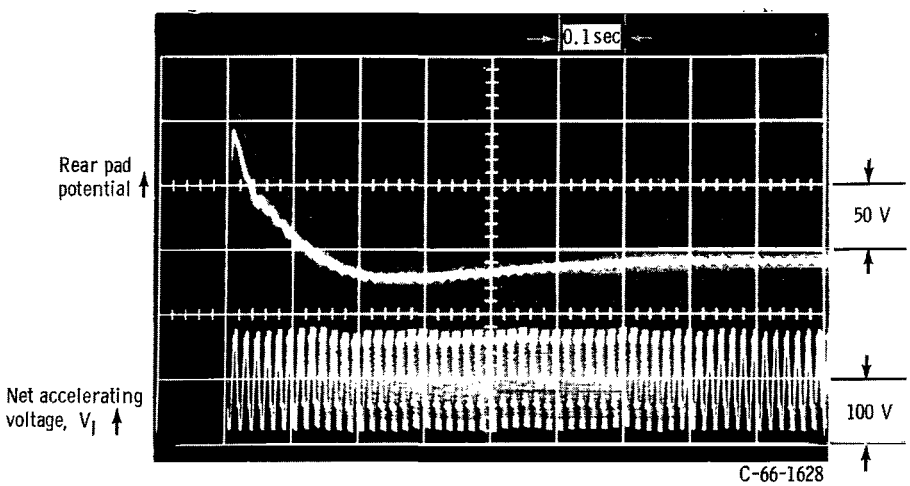

(b) Sweep rate, 10 centimeters per second.

Figure 15. - Oscillograms of rear pad potential and net accelerating voltage. Propellant flow rate, 14.2×10^{-4} gram per second; filament emission current, 2 amperes; accelerator voltage, -2000 volts; direct current level for rear pad potential, 1100 volts; direct current level for net accelerating voltage, 5000 volts.

Voltage and Current Transients

The steady-state leakage current was not strongly correlated with tube breakdown. Transient voltage or current measurements could possibly provide a better insight into the mechanism of sequence of events preceding a sustained discharge. A 2000-ohm carbon resistor was placed in the leakage current circuit and the voltage drop across this resistor was monitored on an oscilloscope (see fig. 4, p. 8). A qualitative comparison of the signal content showed the presence of ion-chamber noise that diminished and disappeared when the ion-chamber discharge was extinguished. This effect would serve to indicate that ions are bombarding the ground electrode. The signal also contained a large amount of background noise and was so poor in quality that the steady-state leakage

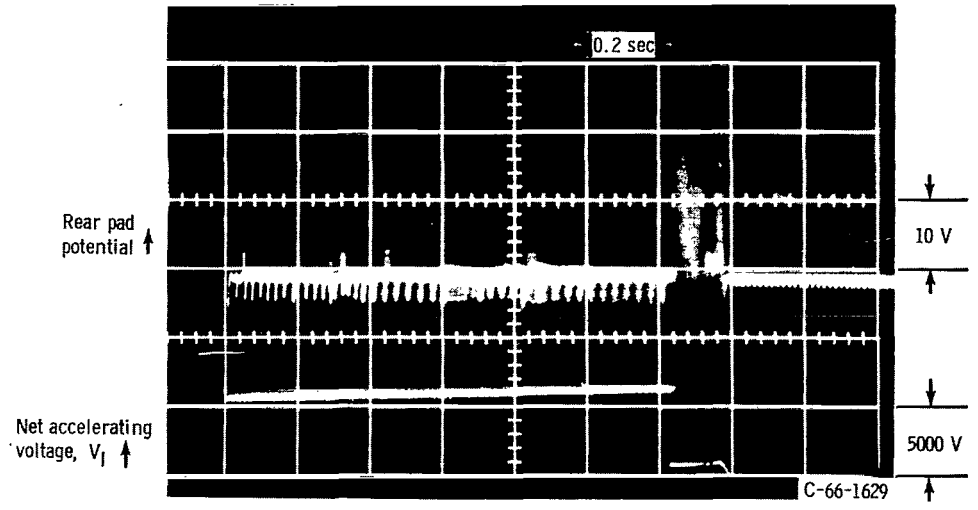

Figure 16. - Oscillogram of voltage-induced breakdown. Sweep rate, 5 centimeters per second; initial net accelerating voltage, 6000 volts; accelerator voltage, -2000 volts; propellant flow rate, 14.2×10^{-4} grams per second; filament emission current, 2 amperes; initial direct current level for rear pad potential, 1300 volts.

current could not be resolved.

Floating potential of the rear pad and the net accelerating voltage were recorded by means of the oscillograms shown in figure 15. Both signals were capacitance-connected to the oscilloscope and thus only the transient components were registered by the signals. The net accelerating voltage was monitored from a 1-megohm voltage divider network. The pad potential was measured with a 100-megohm voltage divider probe (fig. 4, p. 8). The possible current drain through the probe at 1000 volts could be as much as 10 microamperes, which may mask the effects of normal leakage current on tube breakdown.

The oscillogram of figure 15(a) was taken with a sweep rate of 1 centimeter per second at the vertical amplification shown. The broad smear of the net accelerating voltage trace was a 60-cycle ripple. The pad potential contained voltage spikes on the order of 100 volts above a steady-state value of about 1100 volts. The voltage spikes shown were not present at all operating conditions but became more frequent as breakdown was approached. These voltage spikes repeated at a rate of roughly one per second but were not of a fixed frequency. A record of a single voltage spike made at a sweep speed of 10 centimeters per second is shown in figure 15(b). The voltage spike had an extremely fast rise time and an appreciable decay time with some undershoot. The pulse shape resembled the Trichel current of a negative point corona discharge described in reference 9. Although the trace shown is a voltage signal, a spark or a burst of positive charges can cause the potential of an almost isolated pad to rise and to decay at a rate determined by the external circuit impedance through which electrons can flow into the pad.

Tube breakdown discharges occur with explosive suddenness, and transient recording

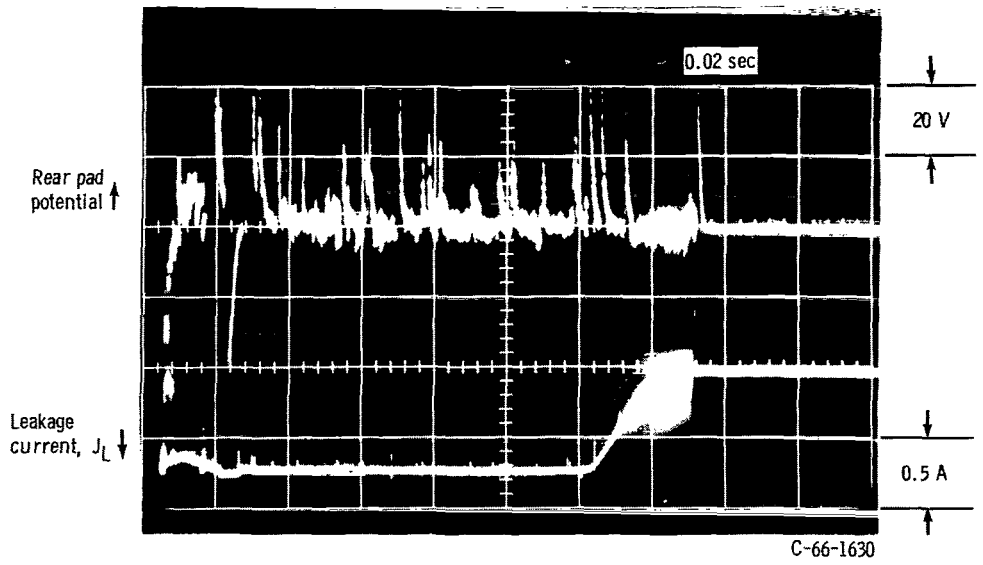

Figure 17. - Spontaneous breakdown during steady-state thrustor operation. Sweep rate, 50 centimeters per second; net accelerating voltage, 7000 volts; accelerator voltage, -2000 volts; propellant flow rate, 14.2×10^{-4} gram per second; filament emission current, 2.0 amperes; direct current level for rear pad potential, 1750 volts.

of events prior to the discharge is extremely difficult. The high oscilloscope sweep rate that must be used requires synchronization not attainable without some predictor signal. A current surge used as a trigger signal is not wholly satisfactory because the discharge has, by then, already begun.

Transients of pad potential and net accelerating voltage monitored during a breakdown induced by steadily increasing the voltage are shown in figure 16. A 4-micromicrofarad capacitor was connected in the circuit between the pad terminal and the voltage divider probe to eliminate direct-current leakage. Starting from 6000 volts, the net accelerating voltage increased to approximately 7000 volts at which point the discharge occurred. The 6500-ohm ballast resistor in the net accelerating voltage circuit caused the voltage to drop about 5500 volts and to maintain a constant tube discharge voltage of about 1500 volts until the circuit breaker opened 0.13 second later. No detectable disturbance occurred in the net accelerating voltage prior to the onset of a discharge. The pad voltage likewise appeared normal until the discharge, at which time rapid voltage fluctuations occurred.

Transient recordings of the pad voltage and leakage current taken during a breakdown that occurred spontaneously while holding a constant net accelerating voltage of 7000 volts are shown in figure 17. The sweep was set at 50 centimeter per second and was triggered from the leakage current signal which appeared as a voltage drop across a 1 ohm resistor. The pad potential trace showed a highly fluctuating signal with voltage spikes on the order of 20 to 40 volts. The leakage current immediately increased to about 750 milliamperes and remained constant until the power supply circuit breaker opened 0.12 second later. The leakage current was limited by the 6500-ohm ballast resistor in the anode circuit,

and the tube discharge voltage was probably about 1500 volts as shown previously in figure 16. The discharge is thus characteristic of an abnormal glow.

The tests described have shown some voltage and current transients related to the operation of the isolation device. The event immediately preceding the discharge, that is, the transition of leakage current from the microampere to the ampere level, could not be obtained with the present instrumentation.

CONCLUSIONS

Observations of a propellant feed tube used as a high-voltage isolation device have given some insight into its characteristics and design principles. Ions from the thrustor are probably responsible for an increased occurrence of secondary processes that leads to a breakdown discharge.

The use of two deionizer pads was effective in reducing the leakage current and presumably the ion density in the tube and especially in the ground electrode region. In addition, the pads may have served to maintain a potential gradient along the tube so that no region exceeded the critical breakdown field corresponding to the local pressure and ion density. Voltages to 10 000 volts could be held within 14.6 centimeters of a grounded surface at a propellant flow rate of 14.2×10^{-4} gram per second and an estimated maximum tube pressure of 0.075 mm Hg.

The specific mechanism and attendant processes during the transition of tube discharge from the microampere level to the self-sustaining breakdown discharge are unresolved. Breakdown generally occurred without prior indication either in leakage current or in net accelerating voltage.

With the present techniques and configurations, isolation of the propellant feed system is possible for most values of thrustor potential of current interest. Sufficient deionizing medium is necessary to assure the desired isolation capability. An optimum design probably exists for each specific application so that the propellant tube size is adequate to handle the required flow rate at an allowable level of tube pressure.

Lewis Research Center,
National Aeronautics and Space Administration,
Cleveland, Ohio, April 15, 1966.

REFERENCES

1. Cobine, James D.: Gaseous Conductors: Theory and Engineering Applications. Dover Publications, Inc., 1958.

2. Loeb, Leonard B.: Secondary Processes Active in the Electrical Breakdown of Gases. Brit. J. Appl. Phys., vol. 3, Nov. 1952, pp. 341-349.

3. Kontaratos, A. N.; and Demetriades, S. T.: Electrical Breakdown of Gases at Elevated Temperatures. Phys. Rev., vol. 137A, no. 6, Mar. 15, 1965, pp. 1685-1686.

4. Brown, Sanborn C.: Basic Data of Plasma Physics. Technology Press of MIT, 1959.

5. Reader, Paul D.: Investigation of a 10-Centimeter-Diameter Electron-Bombardment Ion Rocket. NASA TN D-1163, 1962.

6. Reader, Paul D.: Scale Effects on Ion Rocket Performance. ARS J. vol. 32, no. 5, May 1962, pp. 711-714.

7. Dushman, Saul: Scientific Foundations of Vacuum Technique. John Wiley & Sons, Inc., 1949.

8. Guseva, L. G.: Initiation of a Discharge in Molecular Gases at $pd < (pd)_{min}$. Research in the Field of Electric Discharges in Gases, B. N. Klyarfel'd, ed., All-Union Institute of Electrical Engineering, Transactions (USSR), No. 63, 1958, pp. 1-38. (John Crerar Library Translation No. SLA 60-19079; also as Rep. No. MCL-363/V, Technical Information Center, MCLTD, Wright-Patterson AFB, Ohio.)

9. Trichel, G. W.: The Mechanism of the Negative Point to Plane Corona Near Onset. Phys. Rev., vol. 54, no. 12, Dec. 15, 1938, pp. 1078-1084.

"The aeronautical and space activities of the United States shall be conducted so as to contribute . . . to the expansion of human knowledge of phenomena in the atmosphere and space. The Administration shall provide for the widest practicable and appropriate dissemination of information concerning its activities and the results thereof."

—NATIONAL AERONAUTICS AND SPACE ACT OF 1958

NASA SCIENTIFIC AND TECHNICAL PUBLICATIONS

TECHNICAL REPORTS: Scientific and technical information considered important, complete, and a lasting contribution to existing knowledge.

TECHNICAL NOTES: Information less broad in scope but nevertheless of importance as a contribution to existing knowledge.

TECHNICAL MEMORANDUMS: Information receiving limited distribution because of preliminary data, security classification, or other reasons.

CONTRACTOR REPORTS: Technical information generated in connection with a NASA contract or grant and released under NASA auspices.

TECHNICAL TRANSLATIONS: Information published in a foreign language considered to merit NASA distribution in English.

TECHNICAL REPRINTS: Information derived from NASA activities and initially published in the form of journal articles.

SPECIAL PUBLICATIONS: Information derived from or of value to NASA activities but not necessarily reporting the results of individual NASA-programmed scientific efforts. Publications include conference proceedings, monographs, data compilations, handbooks, sourcebooks, and special bibliographies.

Details on the availability of these publications may be obtained from:

SCIENTIFIC AND TECHNICAL INFORMATION DIVISION

NATIONAL AERONAUTICS AND SPACE ADMINISTRATION

Washington, D.C. 20546